Cell, Vol. 114, 701–713, September 19, 2003, Copyright ©2003 by Cell Press

The Protein Network of HIV Budding

Uta K. von Schwedler,[1] Melissa Stuchell,[1] Barbara Müller,[3] Diane M. Ward,[2] Hyo-Young Chung,[1] Eiji Morita,[1] Hubert E. Wang,[4] Thaylon Davis,[4] Gong-Ping He,[4] Daniel M. Cimbora,[4] Anna Scott,[1] Hans-Georg Kräusslich,[3] Jerry Kaplan,[2] Scott G. Morham,[4] and Wesley I. Sundquist[1,*]

[1]Department of Biochemistry
[2]Department of Pathology
University of Utah
Salt Lake City, Utah 84132
[3]Abteilung Virologie
Universitätsklinikum Heidelberg
D-69120 Heidelberg
Germany
[4]Myriad Pharmaceuticals, Inc.
Salt Lake City, Utah 84108

Summary

HIV release requires TSG101, a cellular factor that sorts proteins into vesicles that bud into multivesicular bodies (MVB). To test whether other proteins involved in MVB biogenesis (the class E proteins) also participate in HIV release, we identified 22 candidate human class E proteins. These proteins were connected into a coherent network by 43 different protein-protein interactions, with AIP1 playing a key role in linking complexes that act early (TSG101/ESCRT-I) and late (CHMP4/ESCRT-III) in the pathway. AIP1 also binds the HIV-1 $p6^{Gag}$ and EIAV $p9^{Gag}$ proteins, indicating that it can function directly in virus budding. Human class E proteins were found in HIV-1 particles, and dominant-negative mutants of late-acting human class E proteins arrested HIV-1 budding through plasmal and endosomal membranes. These studies define a protein network required for human MVB biogenesis and indicate that the entire network participates in the release of HIV and probably many other viruses.

Introduction

HIV spreads via extracellular particles that can enter and exit cells. The characterization of viral and cellular proteins involved in HIV entry has provided a greater understanding of early stages in the viral life cycle, and led to new therapeutics (Biscone et al., 2002). In contrast, the equally important process of HIV release is less well understood, and many of the cellular factors involved in this fundamental stage of the viral life cycle remain to be identified and characterized (for recent reviews see Freed, 2002; Pornillos et al., 2002c).

Efficient HIV release requires the *cis*-acting, tetrapeptide P(S/T)AP "late domain" found in the p6 domain of all HIV Gag proteins, and also in the structural proteins of other pathogenic human viruses including Ebola and HTLV-I (Freed, 2002; Pornillos et al., 2002c). PTAP late domains recruit the cellular protein TSG101 to facilitate virus budding (Demirov et al., 2002a; Garrus et al., 2001; Martin-Serrano et al., 2001; VerPlank et al., 2001). In uninfected cells, TSG101 functions in the biogenesis of the *m*ultive*s*icular *b*ody (MVB) (Katzmann et al., 2002), which suggests that HIV may bind TSG101 in order to gain access to the downstream machinery that catalyzes MVB vesicle budding. Consistent with this model, a dominant-negative Vps4A protein that inhibits MVB biogenesis also blocks release of HIV-1 and other enveloped viruses (Garrus et al., 2001; Licata et al., 2003; Martin-Serrano et al., 2003). The mammalian MVB pathway is not yet fully defined, however. Hence, it is unclear whether other proteins in the MVB pathway participate in HIV-1 budding.

Genetic screens in yeast have defined 17 different proteins that appear to play direct roles in MVB biogenesis (reviewed in Katzmann et al., 2002). All are required for *v*acuolar *p*rotein *s*orting (VPS), and are termed "class E" proteins because their deletion or inactivation induces formation of abnormally enlarged, highly tubulated endosomal membrane compartments that fail to mature normally into MVBs (termed "class E compartments"). Recent studies by Emr and coworkers have revealed that most class E proteins exist predominantly as soluble proteins or subcomplexes that are sequentially recruited from the cytoplasm to function at sites of MVB vesicle formation (termed ESCRTs, for *E*ndosomal *S*orting *C*omplexes *R*equired for *T*ransport) (Babst et al., 2002a, 2002b; Katzmann et al., 2003; Odorizzi et al., 2003). After proteins are sorted into MVB vesicles, the assembled class E proteins are then released upon ATP binding/hydrolysis by the AAA ATPase, Vps4p. Thus, the different factors and stages of yeast MVB biogenesis are now understood in outline. The present studies were undertaken with the goals of defining the network of proteins required for human MVB biogenesis and testing whether HIV-1 budding requires the function of proteins that act later in this pathway.

Results

Modeling the Human Protein Interaction Network Required for MVB Biogenesis

A systematic search for human homologs of yeast class E proteins yielded at least one acceptable match for all 17 yeast proteins, with the exception of Vps37p (Figure 1 and Supplemental Table S1 available at http://www.cell.com/cgi/content/full/114/6/701/DC1). The resulting 22 human proteins can be grouped in analogy to the yeast ESCRT subcomplexes, and the groupings shown in Figure 1A are consistent with studies in mammalian systems indicating that: (1) HRS, STAM1/2, TSG101, and VPS28 all act early in MVB formation (Asao et al., 1997; Babst et al., 2000; Bache et al., 2003a, 2003b; Bishop et al., 2002; Bishop and Woodman, 2001; Lu et al., 2003; Pornillos et al., 2003), and (2) the ESCRT-II proteins

*Correspondence: wes@biochem.utah.edu

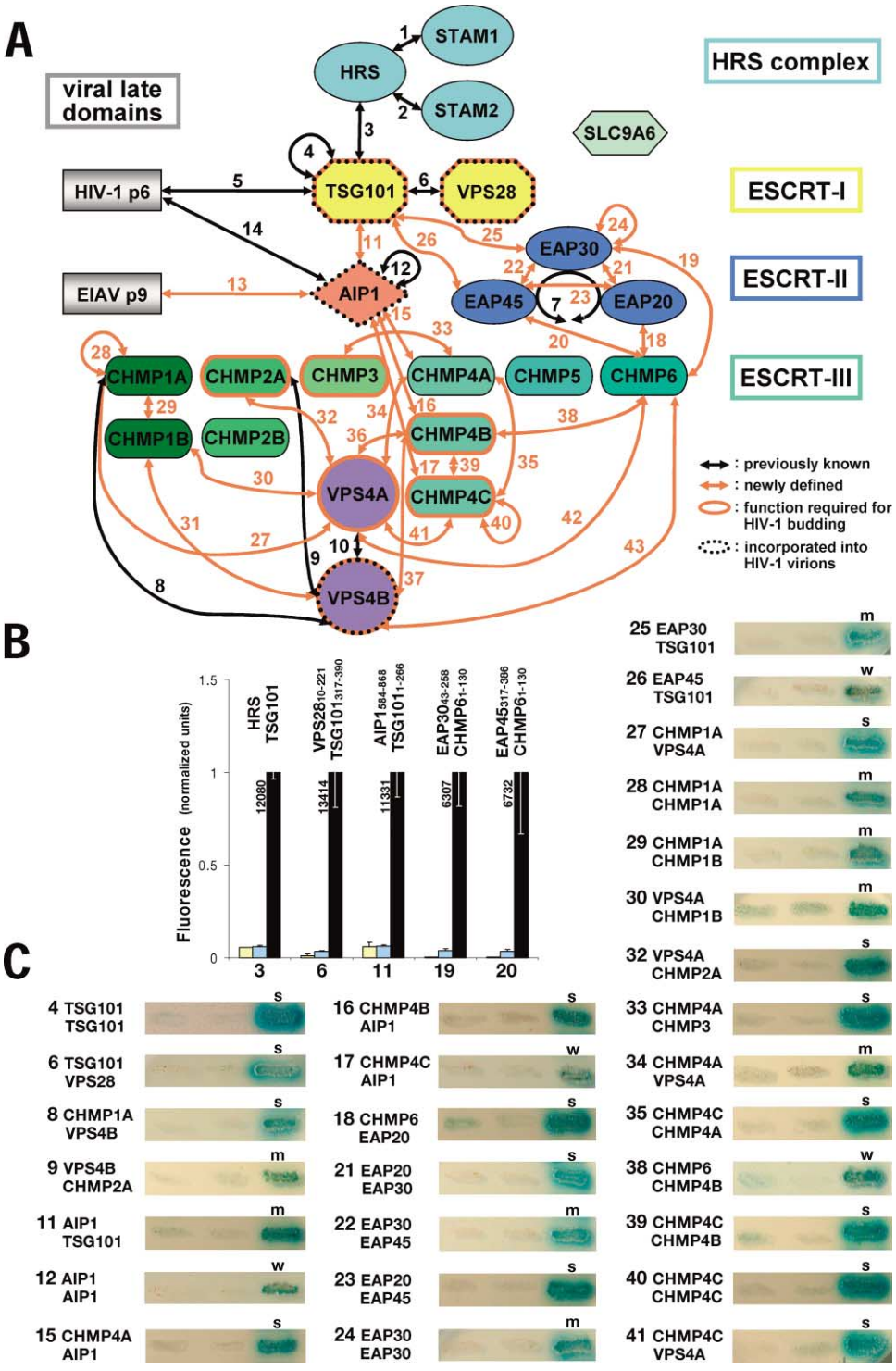

Figure 1. Model for the Human Class E Protein Interaction Network

(A) Schematic illustration showing 22 putative human class E proteins, their subcomplexes, and interactions. Interactions between proteins are denoted by arrows and are color-coded as previously known (black) or novel (red). ESCRT-I, II, III complexes are modeled after analogous yeast complexes (Katzmann et al., 2002). Detection methods, interactions (in brackets) and relevant protein fragments (in parentheses) were: a) Yeast two-hybrid screens of cDNA libraries: [6] ($TSG101_{317–390}$/$VPS28_{10–221}$), [11] ($TSG101_{1–266}$/$AIP1_{584–868}$), [19] ($EAP30_{43–258}$/$CHMP6_{1–130}$), [20] ($EAP45_{317–386}$/$CHMP6_{1–130}$); b) Directed yeast two-hybrid screens [4, 6, 8–9, 11–12, 15–18, 21–30, 32–35, and 38–41] (all full-length proteins); c) Interactions between purified proteins detected using GST pull-down assays: [13] ($AIP1_{1–716}$/EIAV p9), [14] ($AIP_{1–716}$/HIV-1 p6), [16] ($AIP1_{1–716}$/CHMP4B), and [9, 30–32, 36–37, 42–43] (all full-length proteins); d) Interactions between purified proteins detected using Biacore biosensor: [11] ($Tsg101_{1–145}$/$AIP1_{714–723}$). References for previously reported interactions are: [1] and [2] (Asao et al., 1997), [3] (Bache et al., 2003a; Lu et al., 2003; Pornillos et al., 2003), [4] (Martin-Serrano et al., 2003), [5] (Demirov et al., 2002a; Garrus et al., 2001; Martin-Serrano et al., 2001;

form a stable complex in mammalian cells (Kamura et al., 2001).

In several cases, a single yeast protein apparently has two or more human orthologs, implying greater complexity in the mammalian MVB pathway. This is most evident late in the pathway; e.g., the single yeast Vps4p protein has two apparent human orthologs: VPS4A and VPS4B, and the six related proteins of the yeast ESCRT-III class have 10 apparent human orthologs, the *ch*arged *M*VB *p*roteins or CHMP proteins. The six yeast proteins perform distinct functions: two (Vps32p/Snf7p and Vps20p) form a proximal lattice that binds directly to the MVB membrane, two (Vps2p/Did4p and Vps24p) form a distal layer on the first, and the remaining two (Did2p and Vps60p/Mos10p) apparently have partially redundant and/or regulatory roles (Babst et al., 2002a). A phylogenetic analysis showed that the 10 related human CHMP proteins can also be subdivided into six analogous groups (Figure 1A and Supplemental Figure S1 available on *Cell* website).

Protein Interactions within the Human Vps Class E Protein Network

Extensive yeast two-hybrid analyses were performed to test our model for the human MVB pathway and to identify new protein-protein interactions that could link the entire protein network together, which has not been possible in any system including yeast. Potential interactions between human class E proteins were tested using both random library screening and directed yeast two-hybrid assays, which provided overlapping and complementary information (Figure 1, Supplemental Figure S1 and Table S1 available on *Cell* website). In the random screen, early (TSG101) and late (CHMP6) acting class E proteins were used as baits in automated screens of human cDNA libraries, with multiple constructs employed to identify interacting domains. These screens confirmed one previously known TSG101 interaction, TSG101/VPS28 (Bishop and Woodman, 2001), and revealed three novel interactions: TSG101/AIP1, CHMP6/EAP30, and CHMP6/EAP45. All four interactions were confirmed in semiquantitative liquid β-galactosidase two-hybrid assays (Figure 1B).

The directed screen tested for all possible intra- and intermolecular interactions between the 18 human class E proteins predicted to act downstream of TSG101 (including TSG101 itself). A total of 28 interactions were identified and 16 of the 18 proteins tested interacted with at least one other class E protein (Figures 1A and 1C). CHMP5 constructs were toxic or self-activating, and CHMP2B did not show any positive interactions. Our experiments reconfirmed several yeast two-hybrid interactions described previously in mammalian systems: TGS101/TSG101 (Martin-Serrano et al., 2003), TSG101/VPS28 (Bishop and Woodman, 2001), AIP1/AIP1 (Chatellard-Causse et al., 2002), CHMP1A/VPS4B, and CHMP2A/VPS4B (Howard et al., 2001). We also found a series of interactions that were previously undocumented in mammalian systems, but were analogous to interactions previously described in yeast (e.g., CHMP4B/CHMP6, AIP1/CHMP4A-C) (Babst et al., 2002a; Odorizzi et al., 2003), or were consistent with biochemical or genetic experiments in yeast (e.g., ESCRT-I recruits ESCRT-II to the endosomal membrane (Babst et al., 2002b), Snf7p (CHMP4A-C) recruits Bro1p (AIP1) (Odorizzi et al., 2003), and ESCRT-II recruits Vps20p (CHMP6) (Babst et al., 2002b). It is therefore apparent that the MVB pathway is conserved in outline from yeast to man.

Importantly, our two screens revealed 25 new class E protein-protein interactions that had not previously been described in any system. These included the first links between ESCRT-I and ESCRT-II (TSG101/EAP45, TSG101/EAP30), and between ESCRT-I and AIP1 (TSG101/AIP1). Collectively, our data imply a hierarchy of protein interactions required for MVB formation, with HRS complex recruiting ESCRT-I; ESCRT-I recruiting AIP1 and ESCRT-II; AIP1 and ESCRT-II recruiting ESCRT-III; and ESCRT-III recruiting VPS4A/B (see Figure 1A).

TSG101/AIP1 Interactions

The novel interaction between TSG101 and AIP1 detected in the yeast two-hybrid experiments was characterized in greater detail because it provided, to our knowledge, the first direct link between the human ESCRT-I and ESCRT-III complexes. Deletion analyses revealed that the N-terminal UEV domain of TSG101 (residues 1–145) bound the proline-rich C-terminal region of AIP1 (residues 586–868) (Figures 1B and 2A). The TSG101 UEV domain binds specifically to P(S/T)AP sequences, but a mutation in the UEV domain (M95A) abolishes P(S/T)AP binding (Pornillos et al., 2002a, 2002b). The M95A mutation also eliminated AIP1 binding to both the full-length and $TSG101_{1–145}$ proteins (Figure 2A, far right, red bar), indicating that the TSG101 UEV domain bound a P(S/T)AP-like sequence in the proline-rich region of AIP1.

There is a conserved PSAP motif within the proline-rich region of AIP1 (residues 717–720), and we therefore tested whether the TSG101 UEV domain could bind this

VerPlank et al., 2001), [6] (Bishop and Woodman, 2001), [7] (Kamura et al., 2001), [8] and [9] (Howard et al., 2001), [10] (Scheuring et al., 2001), [12] (Chatellard-Causse et al., 2002) and [14] (Strack et al., 2003).

(B) Protein-protein interactions detected in yeast two-hybrid library screens and confirmed using semiquantitative β-galactosidase assays. Positive signals from yeast expressing prey-AD/bait-BD pairs (black bars) are shown together with signals from control cells expressing AD/bait-BD (yellow) and prey-AD/BD pairs (blue). Interaction numbers (below) correspond to those in Figure 1A, and the HRS/TSG101 interaction served as a positive control (Pornillos et al., 2003). Signals were normalized relative to the appropriate positive signal (given in fluorescence units adjacent to black bars).

(C) Directed yeast two-hybrid interactions between human class E proteins detected in X-α-gal assays. From left to right, each image shows X-α-gal signals from yeast patches containing AD/bait-BD (negative control), prey-AD/BD (negative control), and prey-AD/bait-BD (positive interaction). All interactions shown were positive in multiple repetitions of these experiments and are denoted as strong (s, signal in 1–2 days), medium (m, signal in 3 days), and weak (w, signal in 4 or more days). Very weak interactions not scored as positive were: CHMP3/CHMP4B, CHMP1B/VPS4B, CHMP4B/EAP45, and CHMP6/VPS4A. Note that some two-hybrid interactions could be mediated via bridging yeast proteins.

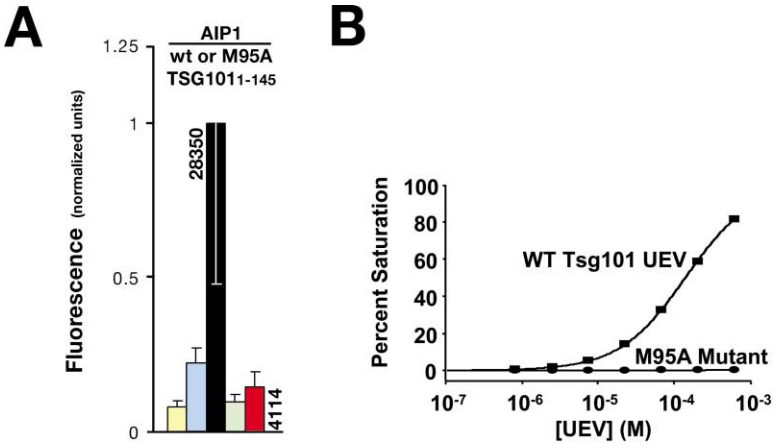

Figure 2. TSG101/AIP1 Interactions

(A) β-galactosidase assays showing two-hybrid interactions between AD/TSG101$_{1–145}$-BD (yellow, negative control), AIP1-AD/BD (blue, negative control), AIP1-AD/TSG101$_{1–145}$-BD (black), AD/M95A-TSG101$_{1–145}$-BD (green, negative control), and AIP1-AD/M95A-TSG101$_{1–145}$-BD (red).

(B) Biosensor binding isotherms for GST-AIP1$_{714–723}$ binding to wt (squares, $K_D = 142 \pm 0.5$ μM) or M95A mutant (ovals) TSG101 UEV. Raw binding data for this figure are given in Supplemental Figure S2A (available on *Cell* website).

motif directly using Biacore biosensor experiments. Pure recombinant TSG101 UEV domain bound specifically to a peptide spanning AIP1 residues 714–723 (denoted AIP1$_{714–723}$; $K_D = 142 \pm 0.5$ μM), and binding was again eliminated by the TSG101 M95A mutation (Figure 2B and Supplemental Figure S2A available on *Cell* website). Hence, the TSG101 UEV domain binds directly to the $_{717}$PSAP$_{720}$ element of AIP1.

AIP1/CHMP4 Interactions

The yeast two-hybrid data also indicated that AIP1 interacts with all three members of the CHMP4 family of ESCRT-III proteins, but not with other CHMP proteins. GST pull-down assays were performed to test for direct, specific protein-protein interactions between AIP1$_{1–716}$ and representatives from 5 of the 6 different CHMP subclasses (1B, 2A, 3, 4B, and 6; GST-CHMP4A, -CHMP4C, and -CHMP5 were poorly soluble and therefore not tested). As shown in Figure 3A, AIP1$_{1–716}$ bound CHMP4B, but not the other CHMP proteins. A single point mutation (L217A) near the C terminus of CHMP4B blocked AIP1 binding (Figure 3A, compare lanes 7 and 8). Although the functional interactions between AIP1 and CHMP4 proteins presumably occur primarily within membrane bound complexes, it was possible to coimmunoprecipitate AIP1-Myc and CHMP4B-FLAG proteins that were overexpressed in 293T cells (Figure 3B). Overall, we conclude that AIP1 binds directly and specifically to the CHMP4 proteins, but not to CHMP proteins from other families.

Interactions of AIP1 and Viral Proteins

Recent evidence suggests that AIP1 may play a direct role in the release of several enveloped viruses, includ-

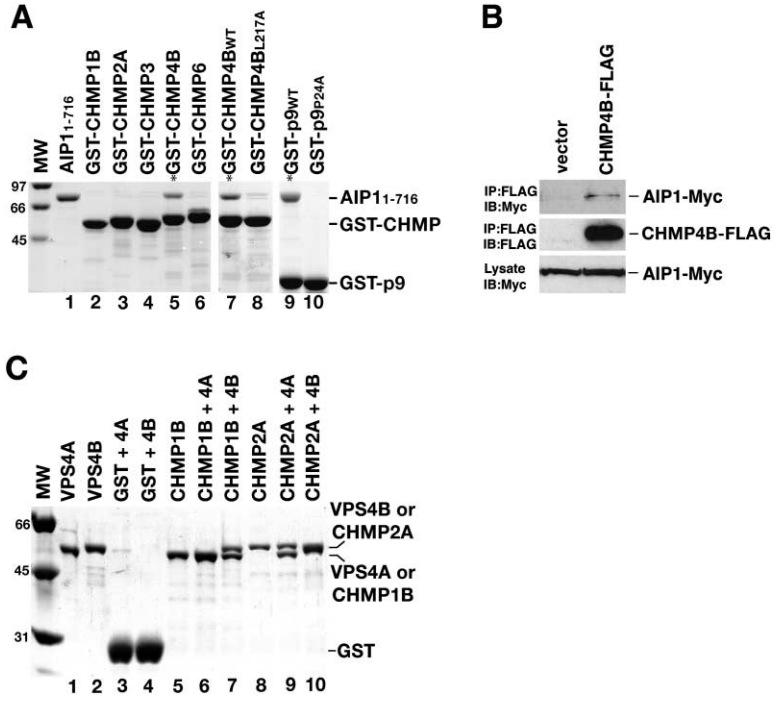

Figure 3. CHMP Protein Interactions

(A) CHMP/AIP1 interactions analyzed in GST pull-down assays. Excess pure AIP1$_{1–716}$ (lane 1, 10% of input) was incubated with glutathione beads prebound with different GST fusion proteins (lanes 2–10, lower bands). Bound AIP$_{1–716}$ was separated by SDS-PAGE and visualized by Coomassie blue staining (upper bands in lanes with asterisks).

(B) Coimmunoprecipitation of CHMP4B and AIP1. 293T cells were cotransfected with AIP1-Myc expression vector and with either pcDNA3.1 control vector (lane 1) or CHMP4B-FLAG expression vector (lane 2). Proteins were immunoprecipitated (IP) from the lysates using anti-FLAG antibodies and detected by Western blotting with anti-Myc (top image) or anti-FLAG (middle image). A Western blot (anti-Myc) of the soluble lysate is shown in the bottom image (1% input).

(C) CHMP/VPS4 interactions analyzed by GST pull-down assays. Pure VPS4A or VPS4B (lanes 1 and 2; 0.7 μg, 5% of input, ~10-fold molar excess) were incubated with glutathione beads prebound with GST alone (lanes 3 and 4), GST-CHMP1B (lanes 6 and 7), or GST-CHMP2A (lanes 9 and 10). GST-CHMP1B and GST-CHMP2A alone are shown in lanes 5 and 8, respectively. Note that GST-CHMP1B/VPS4A and GST-CHMP2A/VPS4B comigrate in lanes 6 and 10, respectively.

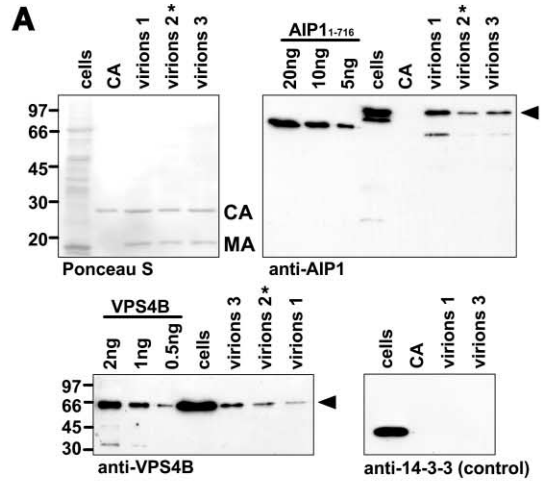

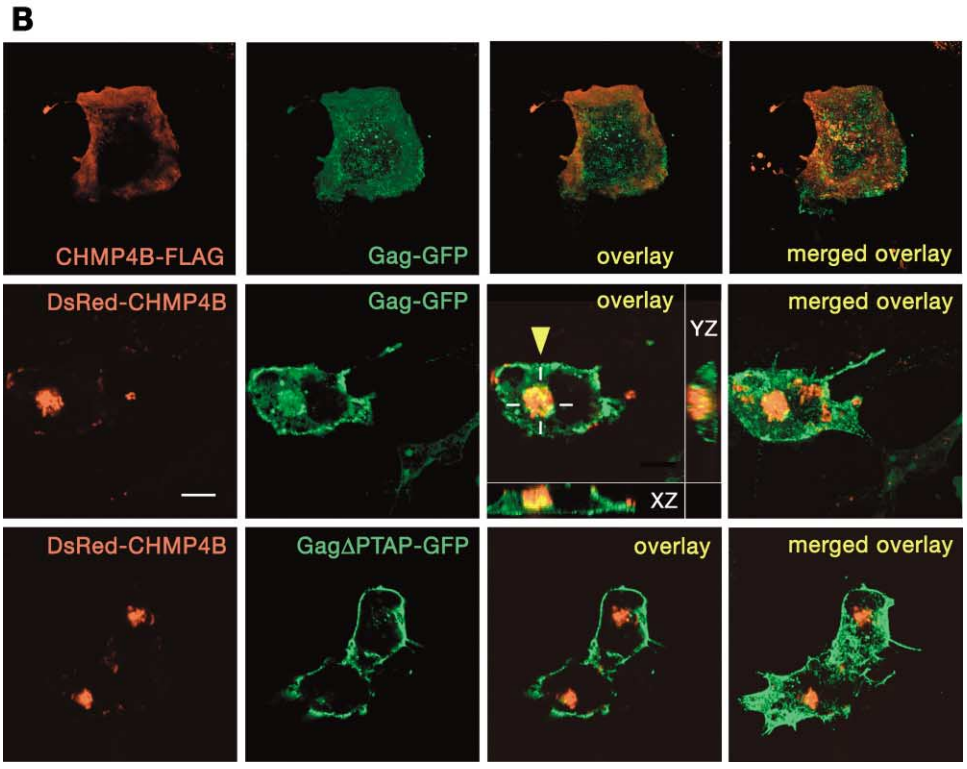

Figure 4. Virion Incorporation and HIV-1 Gag Redistribution to Class E Compartments

(A) Cellular and HIV-1-associated proteins detected by Ponceau S staining (upper left blot) and Western blotting with the indicated antibodies. Lanes labeled "cells" correspond to extracts from 10^5 uninfected MT4 cells (positive control), lanes labeled "CA" correspond to 1 μg pure CA (negative and loading control). Lanes labeled virions 1–3 correspond to independent preparations of purified HIV-1 particles (1 μg CA equivalent), sample 2* was treated with subtilisin. Recombinant $AIP_{1–716}$ and VPS4B protein standards are also shown. Full-length AIP1 protein (arrowhead) is 868 amino acids long, and the presence of multiple bands in the cell and virion lanes presumably reflects multiple protein isoforms, posttranslational modification, degradation products, and/or crossreacting proteins.

(B) Confocal fluorescence microscopic images showing the distribution of CHMP4B (first column, red) and Gag-GFP or GagΔPTAP-GFP (second column, green) in cells expressing CHMP4B-FLAG (top row, negative control) or dominant-negative DsRed-CHMP4B (middle and lower rows). Overlaid red and green images at right show colocalization at the class E compartment of DsRed-CHMP4B with Gag-GFP (yellow arrow). White cross bars mark the directions of the reslicing done in the XZ (bottom inset) and YZ planes (right inset). Single Z-sections are shown in the first three columns, and merged Z-stacks ("merged overlay") are shown in the fourth. Scale bar is 10 μm.

ing HIV-1. As shown above, AIP1 binds directly to TSG101, which in turn binds the $_7$PTAP$_{10}$ late domain of HIV-1 p6^{Gag} and facilitates virus budding. Moreover, Göttlinger and coworkers now report that AIP1 can bind directly to a downstream $_{41}$LRSL$_{44}$ motif within p6 (Strack et al., 2003). We have confirmed their observation and shown that both conserved leucines are required for full affinity AIP1 binding (Supplemental Figure S2B available on *Cell* website). It is therefore likely that Gag forms a ternary complex with both TSG101 and AIP1 during viral

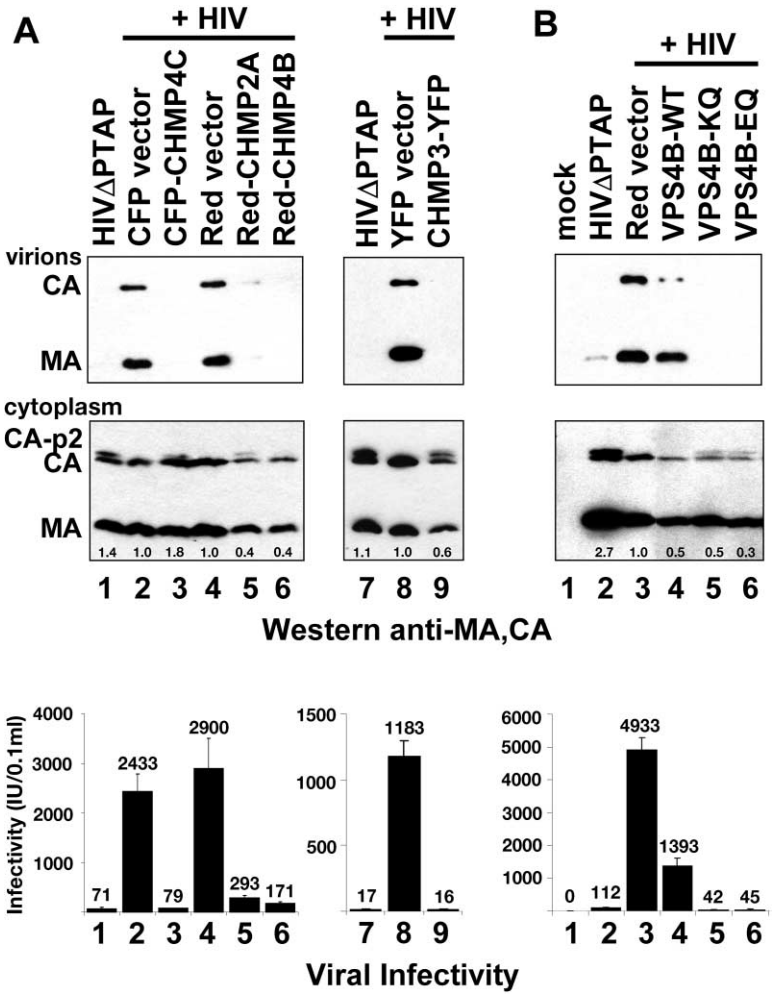

Figure 5. HIV-1 Release and Infectivity Are Inhibited by Dominant-Negative CHMP and VPS4B Proteins

Analyses of HIV-1 Gag protein expression (Western blot, middle image), virion release (top image), and viral infectivity (lower image) in the presence of the dominant-negative CHMP and VPS4B proteins: (A) CFP-CHMP4C, DsRed-CHMP4B, DsRed-CHMP2A or CHMP-YFP and (B) mutant VPS4B proteins. Levels of cytoplasmic Gag proteins relative to the relevant controls were determined by integrating the CA and MA band intensities in lighter exposures (numbers given at bottom of the blot). Note the characteristic late defect in intracellular processing of the CA-p2 protein seen in all cases where virus release is inhibited. Viral titers were determined in single-cycle MAGI infectivity assays of supernatants from transfected cells (blue cells/0.1 ml supernatant).

budding. However, mutations that disrupt the TSG101/Gag interaction typically inhibit HIV-1 release to a much greater extent than do mutations that disrupt the AIP1/Gag interaction, indicating that the class E proteins are probably recruited primarily through the TSG101/Gag interaction (Demirov et al., 2002b; Göttlinger et al., 1991).

It has also been suggested that AIP1 may bind to the YPDL late domain found in the p9 domain of the equine infectious anemia virus (EIAV) Gag (Vincent et al., 2003). Although AP-2 was initially described as a cellular binding partner for the YPDL late domain (Puffer et al., 1998), this has been puzzling because AP-2 functions primarily in endocytosis rather than MVB formation. More recently, however, AIP1 has been proposed as an alternative binding partner for the EIAV late domain because AIP1 orthologs from several organisms can bind YPXL sequences (Vincent et al., 2003). We therefore tested whether AIP1 and EIAV-p9 could form a complex in vitro. As shown in Figure 3A (lane 9), $AIP1_{1–716}$ bound GST-p9 and this interaction was specific for the p9 $_{23}YPDL_{26}$ late domain motif, because binding was abolished (lane 10) by a mutation of the central proline residue (P24A) that also inhibits EIAV release (Puffer et al., 1997). Thus, AIP1 can bind both HIV-1 p6 and EIAV p9, indicating that both viruses enter the mammalian class E protein network, at least in part, through direct interactions with AIP1.

CHMP Proteins Bind VPS4 Proteins

Yeast two-hybrid interactions linked many of the ESCRT-III/CHMP proteins to the two human VPS4 proteins, and we therefore tested whether recombinant VPS4 and CHMP proteins could interact directly. As shown in Figure 3C, pure recombinant mammalian VPS4A and VPS4B proteins bound to GST-CHMP1B (lanes 6 and 7) and GST-CHMP2A (lanes 9 and 10) but not to GST alone (lanes 3 and 4). Analogous VPS4 binding interactions were also seen for the two other CHMP proteins tested (CHMP4B and CHMP6, data not shown). These observations imply that, as in yeast (Babst et al., 2002a), the mammalian VPS4 enzymes likely act directly on the subunits of the CHMP protein lattice.

HIV-1 Packaging and Gag Colocalization of Human Class E Proteins

Cellular factors that participate in viral budding may be packaged into virions, and we have previously shown that the ESCRT-I proteins TSG101 and VPS28 are specifically packaged into HIV-1 virions (J.E. Garrus, K.M. Stray, B.M., H.-G.K., and W.I.S., unpublished data). Proteins that act later in the MVB pathway have not yet been tested for virion incorporation, however. We therefore analyzed purified HIV-1 particles from acutely infected human MT4 cells for the presence of AIP1, CHMP1A,

CHMP2A, VPS4A, and VPS4B. The purity of the virion preparations was evaluated on silver stained SDS-gels (not shown) and by Western blotting, which revealed no detectable contamination with a series of cellular proteins such as the abundant 14-3-3 protein (Figure 4A, bottom right and data not shown; see also Muller et al., 2002).

All of the proteins tested were readily detected in cell extracts (Figure 4A and data not shown). However, only AIP1 and VPS4B were present in multiple independent preparations of HIV-1 particles, with a significantly stronger signal for AIP1 (Figure 4A, lanes labeled virions 1, 2*, and 3). Subtilisin treatment, which degrades proteins on the virion exterior (Ott et al., 2000), did not significantly reduce the AIP1 or VPS4B signals (lanes labeled virions 2*), indicating that these proteins were located inside the viral particles. Absolute levels of virion-associated proteins were estimated by comparing virus-associated CA, AIP1, and VPS4B proteins against known quantities of recombinant proteins. 5–10 ng of AIP1 and 0.1–0.5 ng of VPS4B per μg of CA were detected. Assuming that there are $\sim$5000 Gag molecules per virion (V. Vogt, personal communication), this implies that, on average, 3–12.5 molecules of AIP1 and 0.5–2.5 molecules VPS4B were incorporated into each viral particle.

The PTAP Late Domain Helps Target HIV-1 Gag to Mammalian Class E Compartments

In most cell lines, HIV-1 Gag is released primarily from the plasma membrane, whereas in macrophages the virus buds directly into MVB/late endosomal compartments (Pelchen-Matthews et al., 2003; Raposo et al., 2002). These two observations can be unified by a model in which: (1) Gag is targeted to the late endosome through interactions with the class E proteins; (2) Gag then traffics to the plasma membrane via an endosomal pathway; and (3) viral budding can occur at different stages along this pathway depending on the cell type. This model suggests that HIV-1 Gag may accumulate on endosomal membranes upon arrest of MVB formation, as is the case for the class E proteins themselves (see Supplemental Figure S3 available on *Cell* website).

To test this idea, we examined whether dominant-negative CHMP4B and VPS4B proteins altered HIV-1 Gag-GFP localization. A dominant-negative (DN) VPS4B protein was created by mutating residues required for ATP binding (K180Q) or hydrolysis (E235Q) (see also Fujita et al., 2003), and a dominant-negative CHMP4B protein was created by fusing DsRed to the protein's N terminus (Howard et al., 2001). The expected class E phenotypes induced by expression of VPS4B-K180Q, VPS4B-E235Q, and DsRed-CHMP4B were confirmed in a series of control experiments showing that: (1) the DN VPS4B proteins inhibited ligand-induced lysosomal degradation of surface MHC-I and EGFR proteins (Supplemental Figure S3A–S3F available on *Cell* website); (2) the DN VPS4B and CHMP4B proteins induced formation of aberrantly enlarged, vacuolated "mammalian class E" compartments that stained positive for both lysosomal and endosomal markers (Supplemental Figure S4 available on *Cell* website); and (3) the soluble, nondominant-negative CHMP4B-FLAG protein relocalized to the class E compartments induced by expression of the DN VPS4-E235Q protein (Supplemental Figure S4 available on *Cell* website).

Gag-GFP redistributed significantly from the plasma membrane/cell periphery into class E compartments upon expression of either DsRed-CHMP4B (Figure 4B) or VPS4B-E235Q (data not shown). Similar results were obtained for dominant-negative versions of the CHMP2A and VPS4A proteins (data not shown). Moreover, the degree to which Gag-GFP redistributed apparently depended upon TSG101 binding to Gag, as colocalization of wt Gag-GFP/DsRed-CHMP4B was observed in 68% of the cells examined ($n = 19$), whereas colocalization of mutant GagΔPTAP-GFP/DsRed-CHMP4B was uncommon (18%, $n = 48$; Figure 4B, bottom image). Our data therefore support a model in which nonfunctional CHMP and VPS4 proteins cause Gag proteins to accumulate together with TSG101 and other trapped class E proteins on the surface of aberrant late endosomal compartments.

Dominant-Negative CHMP and VPS4B Proteins Block HIV-1 Release and Infectivity

The functional involvement of the CHMP and VPS4B proteins in HIV-1 release was also tested using dominant-negative proteins. A DN CHMP1A protein can be created by fusing large polypeptides to the protein's C terminus (Howard et al., 2001). We found, however, that many such CHMP fusion constructs were cytotoxic and reduced Gag protein expression. We therefore surveyed a series of 25 N- and C-terminal CHMP fusion proteins for the ability to inhibit virus release without strongly reducing Gag expression (see Supplemental Table S2 available on *Cell* website).

As shown in Figure 5A, HIV-1 release was dramatically inhibited by coexpression with CFP-CHMP4C, DsRed-CHMP2A, DsRed-CHMP4B, and CHMP3-YFP. Virus release was analyzed by: (1) Western blot detection of virion-associated MA and CA proteins released by cells expressing HIV-1 (upper images), and (2) reductions of viral titers in single cycle MAGI assays (lower images). Intracellular Gag protein expression was analyzed by Western blot detection of cytoplasmic MA and CA proteins (middle images). Controls for these experiments included the appropriate empty vectors (negative controls) and HIVΔPTAP mutants (positive controls for arrested HIV-1 budding).

The most dramatic effects were observed for the CFP-CHMP4C construct, which did not alter cellular Gag expression levels, but reduced virus release to nearly undetectable levels in the Western blot assay and reduced the release of infectious virus more than 30-fold. DsRed-CHMP2A, DsRed-CHMP4B, and CHMP3-YFP also reduced viral infectivity significantly (10-, 17-, and 73-fold, respectively), albeit with modest reductions in Gag protein expression (2- to 3-fold).

Coexpression of the dominant-negative VPS4B proteins inhibited virus release $>$100-fold for both mutants (Figure 5B), although Gag expression levels were again reduced modestly (2- to 3-fold in the Western blot assay, middle image). In contrast, the wt VPS4B (negative control) produced a comparable 2-fold reduction in cellular Gag expression levels, but with no additional reduction

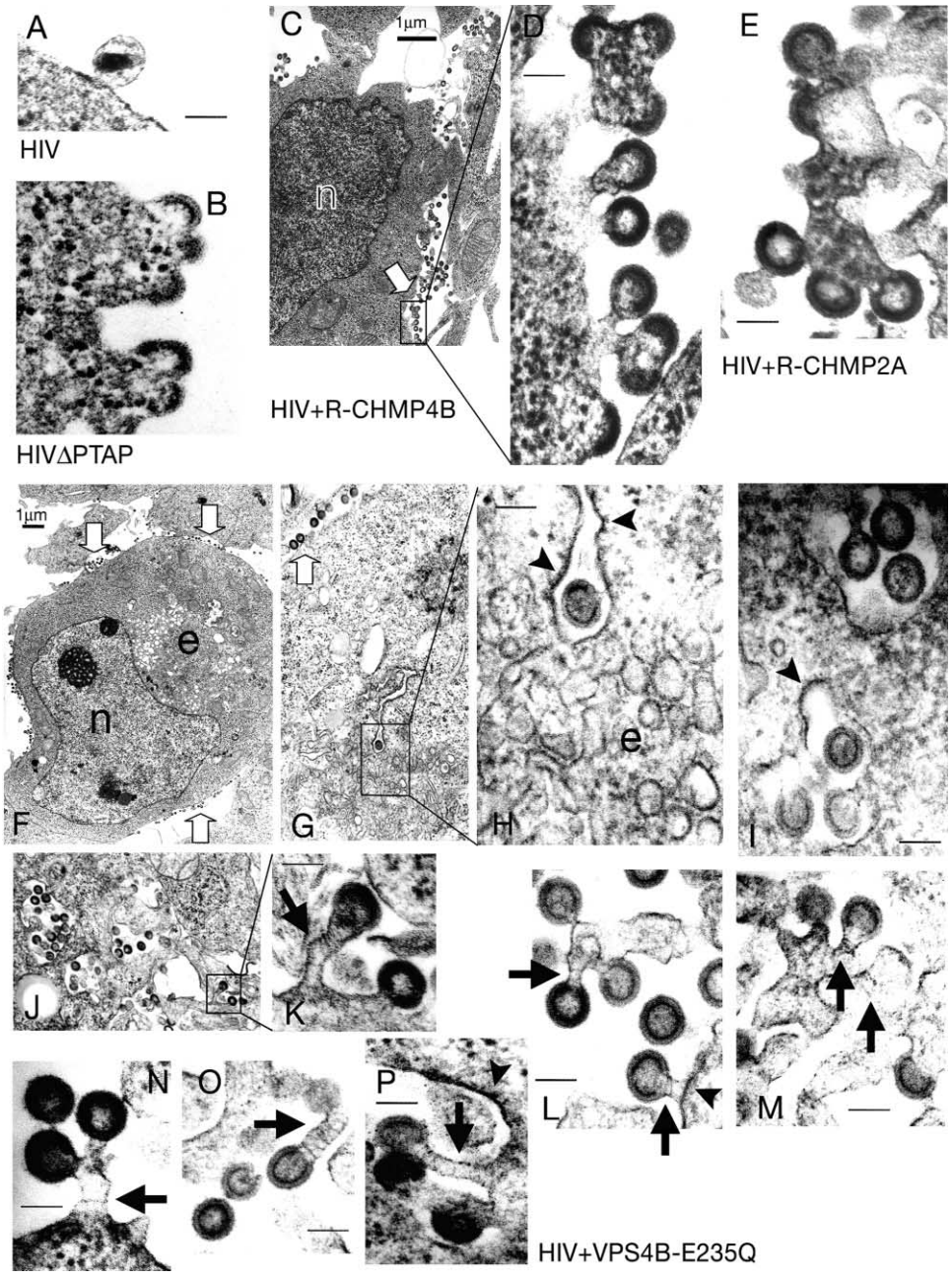

Figure 6. HIV-1 Budding Arrest Induced by Dominant-Negative CHMP and VPS4B Proteins

EM images of thin-sectioned 293T cells transfected with HIV alone (A), HIVΔPTAP (B), or HIV and dominant-negative DsRed-CHMP4B (C and D), DsRed-CHMP2A (E), or DsRed-VPS4B-E235Q (F–P). Thick scale bars are 1 μm; thin scale bars are 100 nm. Open arrows indicate virions arrested in budding at the plasma membrane; arrowheads indicate thickened protein coats on plasma or endosomal membranes; and black arrows indicate striations in the stalks of arrested virions. n: nucleus; e: highly vacuolated class E compartment.

in viral titer (3.5-fold). These data demonstrate that the dominant-negative CHMP and VPS4 proteins diminish particle release and infectivity very significantly, indicating that they likely play a functional role in HIV-1 release.

Dominant-Negative VPS4B and CHMP Proteins Arrest HIV-1 Budding at a Late Stage

Electron microscopy was used to determine the stage at which virus release was arrested by the dominant-negative CHMP2A, CHMP4B, and VPS4B proteins. Thin-sectioned 293T cells transfected with wt HIV-1 DNA alone displayed very few cell-associated virions, and these typically exhibited the conical viral cores that are the hallmark of the mature infectious virus (Figure 6A). In contrast, coexpression of HIV-1 with dominant-negative DsRed-CHMP2A, DsRed-CHMP4B, or VPS4B proteins caused viruses to arrest at a very late stage in assembly, in which extensive clusters of immature particles accu-

mulated at the plasma membrane but remained connected via membrane stalks (Figure 6, open arrows). This arrest resembled a late domain phenotype, except that GagΔPTAP mutants frequently arrested at a somewhat earlier stage (often following membrane distortion, but prior to stalk formation; Figure 6B and see Garrus et al., 2001), suggesting that virus release may proceed through multiple stages and that the dominant-negative VPS4B, CHMP4B, and CHMP2A proteins inhibited a very late step(s) in release.

Cells coexpressing HIV-1 and VPS4B-E235Q proteins exhibited aberrant clusters of tubules and vacuoles that were not observed in control cells. These presumably corresponded to the class E compartments seen by fluorescence microscopy (Figures 6F–6H, labeled "e" and see Supplemental Figure S4 available on *Cell* website). Strikingly, we frequently observed HIV particles arrested in the process of budding into the vacuoles associated with these compartments (Figures 6G and 6H) as well as into other, smaller clusters of intracellular vacuoles (Figures 6I, 6J, and 6P). Viruses arrested while budding through intracellular and plasma membranes were morphologically indistinguishable, and we therefore conclude that VPS4B-E235Q imposes similar blocks at internal and external membranes.

The size and appearance of the internal compartments varied considerably, as did the morphologies of the arrested virions (e.g., in content and in stalk length and width). Nevertheless, there were two indications that cellular protein complexes might be functioning at the sites of viral budding. Firstly, we and others often observed a thickening of the cytoplasmic faces of membranes near sites of virus budding, which may correspond to the ESCRT-III protein coat (see Figures 6H, 6I, 6L and 6P, arrowheads) (Pelchen-Matthews et al., 2003). Secondly, ring-like striations were sometimes observed within the membrane stalks of viruses arrested by the dominant-negative VPS4B-E235Q protein (Figures 6K–6P, highlighted by black arrows). These striations were not observed for ΔPTAP viruses (which are presumably defective in recruiting TSG101 and other class E proteins and rarely showed narrow membrane stalks). We therefore speculate that the membrane coats and/or striations may represent trapped cellular machinery that might normally help to catalyze protein sorting, membrane fission, and/or virus release from wild-type cells.

Discussion

Our experiments define the human class E protein network and strongly support the idea that HIV-1 utilizes this entire network during viral egress (see Figure 7). Most importantly, HIV-1 release can be arrested at a late stage by deletion or mutation of at least 8 different human class E proteins, which function both early (TSG101, VPS28) (Garrus et al., 2001; Martin-Serrano et al., 2001, 2003), and late (CHMP2A, CHMP3, CHMP4B, CHMP4C, VPS4A, VPS4B) in the MVB pathway. In addition, HIV-1 particles package multiple copies of proteins that act both early (TSG101, VPS28), and later (AIP1) in the MVB pathway. They are also enriched in at least one protein that functions very late in the pathway (VPS4B),

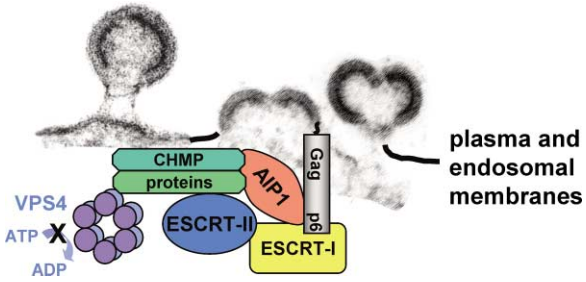

Figure 7. Schematic Model for the HIV-1 Budding Arrest Induced by Expression of Dominant-Negative VPS4 Proteins

The illustration emphasizes how nascent viral particles arrest together with class E protein complexes at both endosomal and plasma membranes when VPS4 proteins are unable to hydrolyze ATP (denoted by the black X). Proteins and complexes are color-coded as in Figure 1A. The figure is simplified in that oligomeric proteins are represented only once (e.g., Gag, TSG101, AIP1, and CHMP proteins), only the plasma membrane arrest is shown, and many temporal and spatial details of the illustrated interactions remain to be elucidated.

indicating that VPS4B acts near sites of viral assembly and release. Although additional studies will be required to understand HIV-1 release in molecular detail, the apparent requirement for more than 20 cellular proteins in this essential viral process provides many potential new targets for therapeutic intervention.

Our studies also begin to define the different roles of human class E proteins in MVB biogenesis. As in yeast, human CHMP6 appears to be recruited by the ESCRT-II complex, whereas the CHMP4 proteins are recruited by AIP1 (see Figures 1 and 7) (Babst et al., 2002b; Odorizzi et al., 2003). Importantly, we also found that TSG101 and AIP1 make a series of key interactions along the MVB pathway: HRS/TSG101→TSG101/EAP30,45; TSG101/AIP1→AIP1/CHMP4A-C that collectively link the human HRS, ESCRT I, II, and III complexes (Bache et al., 2003a; Pornillos et al., 2003, and this work).

It is striking that the UEV domain of TSG101 can bind to PTAP motifs found in three different proteins in the pathway (HRS, TSG101 itself, and AIP1) (Bache et al., 2003a; Katzmann et al., 2003; Lu et al., 2003; Pornillos et al., 2003) as well as in the HIV-1 $p6^{Gag}$ protein (Demirov et al., 2002a; Garrus et al., 2001; Martin-Serrano et al., 2001; VerPlank et al., 2001). TSG101 could, in principle, bind multiple partners simultaneously as it self-oligomerizes in two-hybrid assays (Figures 1A and 1C). Alternatively, TSG101 may bind sequentially to the different PTAP elements, producing conformational changes that could give directionality to the pathway. In either case, we speculate that viral protein binding to the recognition domains of TSG101 and AIP1 may serve not only to recruit the machinery of vesicle formation, but also to alter normal protein-protein interactions required during protein sorting and MVB vesicle formation. This could activate the vesicle fission machinery and/or allow viral proteins to substitute for cellular protein cargos.

Although it is not yet clear where HIV-1 Gag first meets (or recruits) the human class E proteins, the retroviral Moloney Murine Leukemia Gag protein traffics along endosomal membranes before appearing at the plasma

membrane (Basyuk et al., 2003). Moreover, several groups have demonstrated that in macrophages, HIV-1 buds primarily into intracellular compartments that correspond to multivesicular bodies (Pelchen-Matthews et al., 2003; Raposo et al., 2002). Our studies also support a role for endosomal compartments in both Gag trafficking and virus budding. Specifically, we find that even in nonmacrophage lineages (293T cells), where viruses seem to bud predominantly from the plasma membrane, induction of a class E phenotype causes HIV-1 Gag to concentrate and arrest while budding into class E compartments.

Intracellular budding is particularly noticeable under class E conditions because arrested viral particles accumulate on membranes, and possibly also because the trapped class E proteins may recruit Gag more efficiently than in wild-type cells (where the class E proteins are predominantly cytosolic). Nevertheless, we and others (Sherer et al., 2003; M. Thali, personal communication) have observed intracellular HIV-1 budding even in wild-type 293T cells, particularly with the HIVΔPTAP mutant (which again facilitates visualization because the viruses arrest while budding). Conversely, we (and many others) have observed wt virus in the process of budding directly from the plasma membranes of 293T and HeLa cells (e.g., see Supplemental Figure S5 available on *Cell* website). It therefore appears that HIV-1 can bud into both internal endosomal and plasma membranes, and the degree to which the alternate sites are utilized in different cell types may simply reflect differences in the relative rates of virus budding versus Gag trafficking to the plasma membrane. Importantly, virions that bud into intracellular compartments can still emerge from the cell via the exosome pathway, i.e., when the limiting MVB membranes fuse with the plasma membrane and release their vesicles (or viruses) as exosomes (Denzer et al., 2000; Pornillos et al., 2002c; Raposo et al., 2002). The parallels between exosomes and viruses are further emphasized by the fact that AIP1 and TSG101, as well as MLV Gag proteins, are found in preparations of murine exosomes (Thery et al., 2001). A full discussion of the potential relationships between exosomes and viruses is given in Gould et al. (2003).

It will be of interest to understand what factors influence where the virus buds, how Gag traffics via the endosomal network to the plasma membrane, and whether viruses can control these events. These issues could impact viral pathogenesis because endosomal pathways could be used to promote directional release (e.g., see Igakura et al., 2003; McDonald et al., 2003) and because the primary sites of virus release likely change during AIDS disease progression as the tropism of the virus evolves from macrophages (internal budding) to T cells (plasma membrane budding).

A final important finding implied by this and related work is that multiple different classes of enveloped viruses exit cells via the same MVB pathway. In support of this idea, two human class E proteins (AIP1 and TSG101) bind directly to structural proteins from two different viruses (HIV-1 p6/TSG101/AIP1 and EIAV p9/AIP1) and link them directly into the MVB pathway. Moreover, a dominant-negative VPS4A protein that induces a class E phenotype blocks the release of viruses that bud via all known late domains (PTAP, PPXY, YPDL, and/or LXXL) (Garrus et al., 2001; Martin-Serrano et al., 2003).

In conclusion, multiple classes of enveloped viruses utilize the unique budding topology of MVB vesicles as a nonlytic mechanism for escaping cells. Here, we have identified an extensive network of human proteins involved in both cellular protein trafficking and virus release, setting the stage for understanding how these proteins help catalyze protein sorting, membrane deformation, and fission from the cytoplasmic face of a budding vesicle or virus.

Experimental Procedures

Yeast Two-Hybrid Experiments

Directed two-hybrid assays with full-length human class E genes (Supplemental Table S1 available at *Cell* website) were performed using the Matchmaker GAL4 Yeast Two-Hybrid 3 system (Clontech). Library screening was performed as described (Garrus et al., 2001), with eleven different TSG101 and four different CHMP6 baits screened against 3-11 $\times$ 10^6 activation domain (AD) fusions derived from human spleen, brain, and macrophage cDNA libraries.

Two-hybrid interactions were tested in -Leu, -Trp, -Ade, -His, X-α-gal (50 μg/mL) plate assays (Figure 1C) or in semiquantitative liquid culture β-galactosidase activity assays (Figure 1B). In liquid assays, yeast transformants were picked and grown in 100 μl (-Leu, -Trp) SD media in 96 well flat-bottomed plates to an average A_{610} of $\sim$0.4. Resorufin β-D-galactopyranoside (RDG) assay solutions were 1:1 mixtures of: (1) 25 mM PIPES, [pH 7.2]; 10 mM RDG, and (2) 250 mM PIPES, [pH 7.2]; 10% NP-40; 0.24 Units/ml lyticase. 20 μl of the RDG mix was added to each well, and fluorescence was measured after 0 and 1–2 hr of incubation at 37°C (SpectraMAX GeminiXS, Molecular Devices, Inc. Sunnyvale, CA; excitation at 566 nm, emission at 628 nm, with a 610 nm cutoff filter).

Protein Expression and Purification

Expression Constructs

The EIAV p9 gene was PCR-amplified as an NdeI–BamHI-fragment from a proviral $EIAV_{UK}$ plasmid (a gift from Frank Cook, University of Kentucky) (Cook et al., 1998). Other genes were amplified by PCR (with the first 5 codons optimized for *E. coli* expression) from templates listed in Supplemental Table S1 (available on *Cell* website). Genes were subcloned into the NdeI/BamHI sites of a modified pGEX2T vector (WISP01-69, for GST fusion proteins) or pET11a (Novagene, for $AIP1_{1–716}$) and verified by sequencing. $AIP1_{1–716}$ lacked the proline-rich region, which hindered expression of full-length AIP1. Mutations were introduced by PCR megaprimer mutagenesis.

Protein Expression

BL21(DE3) *E. coli* cells were grown to mid log, induced with 0.5 mM IPTG, and recombinant proteins were allowed to accumulate for 2–4 hr (23°C). Cells were harvested, lysed using lysozyme (10 μg/l culture) and sonication, and insoluble material was removed by centrifugation (30 min at 25,000 $\times$ g).

GST fusion proteins were purified by glutathione affinity chromatography, cleaved to remove glutathione, and repurified by conventional chromatography (Pornillos et al., 2002a). Untagged $AIP1_{1–716}$ was precipitated with 55% saturated ammonium sulfate after a 27% precut, redissolved in 25 mM MOPS [pH 7.0], 5 mM β-ME, and purified by Q-Sepharose chromatography (Amersham Pharmacia; elution at $\sim$250 mM NaCl from a linear gradient of 0–1 M over 400 mL). Fractions containing $AIP1_{1–716}$ were pooled, adjusted to 1 M ammonium sulfate, and purified by phenyl-Sepharose chromatography (Amersham Pharmacia; pure $AIP1_{1–716}$ eluted at $\sim$80 mM ammonium sulfate from a linear gradient of 1–0 M over 200 ml). Mass spectrometry confirmed the identity of $AIP_{1–716}$ (minus the N-terminal methionine). Yields were typically 20 mg $AIP_{1–716}$ per liter culture. The expression and purification of human VPS4 proteins will be described elsewhere (A.S., F.G. Whitby, W.I.S., and C.P. Hill, unpublished data).

Protein Interactions

Biosensor Measurements

Binding affinities of pure Tsg101 UEV domains to immobilized GST-AIP1$_{714–723}$ (AREPSAPSIP) were quantified using a Biacore biosensor (20°C in 20 mM sodium phosphate, 150 mM NaCl, 0.01% P20, 50 μg/mL BSA, [pH 7.2]) (Garrus et al., 2001).

GST Affinity Cochromatography

GST-CHMP fusion proteins used in affinity cochromatography (pull-down) assays (Figure 3) were expressed from pGEX vectors in BL21(DE3) *E. coli*, prebound to glutathione agarose (Amersham-Pharmacia), and tested for binding to AIP1$_{1–716,}$ VPS4A, or VPS4B following manufacturer's instructions.

Immunoprecipitations

293T cells (10 cm plate) were cotransfected (Lipofectamine 2000, Invitrogen) with 6 μg pcAIP1-Myc expression vector (see below) and 6 μg CHMP4B-FLAG or control vector (modified from pcDNA3.1). Cells were harvested (24 hr), lysed for 30 min on ice in 20 mM Tris·HCl [pH 7.4], 150 mM NaCl, 0.5% NP-40, with 2 μM pepstatin, 1 mM PMSF, 10 μg/mL leupeptin, 5 μg/mL aprotinin, and clarified by centrifugation (16,000 × g for 30 min). Lysate (1 mg total protein) was incubated (3 hr, 4°C) with 1 μg of anti-FLAG antibody (M2, Sigma) and antimouse IgG rabbit antibody (Zymed) conjugated to Protein A Sepharose (Amersham Bioscience). Unbound proteins were removed by washing with lysis buffer, and bound proteins analyzed by Western blotting with anti-FLAG (1:5000; Sigma M2) or anti-Myc antibodies (clone 9E10, 1:1000, Covance Inc.).

Antibody Production

Antibodies to recombinant AIP1$_{1–716}$ (sera UT324 + UT325), CHMP2A (UT318), VPS4A (UT289), and VPS4B (UT292) were raised in New Zealand White Rabbits (Covance Inc.). Affinity columns were prepared with 1 mg of purified GST fusion proteins coupled to NHS-activated crosslinked agarose (1 ml HiTrapTM NHS-activated HP column, Amersham Biosciences) following manufacturer's instructions. Antiserum (1 mL) was applied to PBS-equilibrated columns, incubated (1 hr, 23°C), and washed with 10 ml PBS. Bound antibody was eluted in 50 mM glycine, 150 mM NaCl, [pH 2.5], neutralized immediately by addition of 0.2 M Tris·HCl, [pH 8.0], concentrated using Vivaspin 0.5 ml concentrators (Vivascience) and dialyzed against PBS. Anti-CHMP1A was a gift from Dan Stauffer.

Detection of Proteins Incorporated into HIV-1 Particles

Human MT4 cells were infected with HIV-1$_{NL4-3}$ by coculture as described previously (Welker et al., 2000). Culture medium was harvested and virus purified by pelleting through a 20% (w/w) sucrose cushion followed by velocity centrifugation through an iodixanol gradient (Dettenhofer and Yu, 1999) and concentration by ultracentrifugation. Subtilisin treatment was performed on virus preparation 2 following the initial 20% sucrose cushion (Ott et al., 2000). For Western blots, virus particles corresponding to 1 μg CA (adjusted by comparison with purified recombinant CA protein) (Gross et al., 1997) were separated by 15% SDS-PAGE (acrylamide:bisacrylamide 200:1) and compared to 1 μg recombinant CA (negative and loading control) and to extracts from 10^5 uninfected MT4 cells. Proteins were transferred to nitrocellulose and detected by ECL using Super Signal West Pico (Pierce) according to manufacturer's instructions. Primary antibodies used were affinity purified anti-VPS4B (1:500) and anti-AIP1 (1:250) sera, or polyclonal anti-14-3-3γ (C-16, Santa Cruz Biotechnology; 1:1000), respectively.

Mammalian Expression Constructs

For DsRed-VPS4B expression, DNA encoding VPS4B was amplified from pGEX-VPS4B by PCR and cloned into the EcoRI/BamHI sites of pDsRed2-C1 (Clontech). VPS4B mutations were introduced by PCR megaprimer mutagenesis, with mutant primers introducing a KpnI site (K180Q) or ClaI site (E235Q), respectively. CHMP genes were cloned into the same sites of pDsRed-C1, pDsRed-N1, pEGFP-C1, pCFP-C1, and/or pYFP-N1 (Clontech), and in pcDNA3.1(−)/Myc-HisA (Invitrogen) either with C-terminal FLAG tags or as fusions with the vector Myc tags (see Supplemental Table S2 available on *Cell* website). AIP1 was cloned into pcDNA3.1(−)/Myc-His. Full cloning details are available upon request. Expression vectors for HIV-1$_{NL4-3}$ (R9 and R9ΔPTAP), Gag-GFP (a gift from Marilyn Resh), and GagΔ-PTAP-GFP have been described (Garrus et al., 2001; Hermida-Matsumoto and Resh, 2000)

Immunofluorescence

COS-7 cells growing on glass cover slips in 60 mm dishes (in DMEM/10% FBS) were transfected with 2 μg plasmid DNA and 12 μl GeneJammer (Stratagene) as per manufacturer's instructions. Twenty-four hr posttransfection, cells were fixed in 3.7% formaldehyde/PBS and permeabilized in 0.1% Triton X-100/PBS/1%BSA. Cells were incubated with either rabbit anti-M6PR (1:200, from Peter Lobel) or mouse anti-Lamp-2 (1:200, Developmental Hybridoma) at 23°C for 60 min. Samples were washed and incubated with goat antirabbit or antimouse Alexa 488-conjugated antibodies (1:750, Molecular Probes). FLAG-tagged CHMP4 proteins were detected using Alexa 488-or Alexa 594-congugated anti-FLAG (1:750, Sigma M2). Images were collected as single wavelengths on an Olympus FVX confocal fluorescent microscope with a 60× Pianapo objective (1.4 NA oil), using Fluoview 2.0.39 software. 0.5 μm thick Z sections or merged Z stacks are shown. Reslicing and three-dimensional representation of Z sections were created with Volocity imaging software (Improvision).

HIV Protein Expression in 293T Cells

For Western blots of Gag expression, infectivity assays and EM, 293T cells in 6-well plates were transfected with 9 μl Lipofectamine 2000 (Invitrogen) per 2 μg HIV-R9 + 1 μg other expression vectors per well as described (Garrus et al., 2001).

Gag Western Blots and Viral Replication Assays

Cytoplasmic proteins and sucrose-pelleted virions (Figure 5) were harvested 36 hr after transfection, resolved by 12% SDS-PAGE, blotted, and detected by ECL as described (von Schwedler et al., 1998). Primary antibodies were rabbit anti-CA #40 at 1:2000 and rabbit anti-MA at 1:20,000. HIV infectious titers were assayed by MAGI assays in P4 cells (von Schwedler et al., 1998).

Electron Microscopy

For EM studies, transfected 293T cells were fixed, stained, and embedded in Spurr's plastic 48 hr after transfection (Garrus et al., 2001), and EM images were obtained at magnifications of 5000–150,000×.

Acknowledgments

We thank Cynthia Lodding, Mimi Payne, Collin Kieffer, and Sanaz Ghaffarian for cloning and technical assistance; David Myszka and the University of Utah Protein Interactions facility for Biacore biosensor measurements; Chris Rodesh for confocal microscope training; and Mark Marsh and Heinrich Göttlinger for sharing their unpublished manuscripts. This work was supported by NIH grants to W.I.S. and J.K.

Received: May 13, 2003
Revised: August 22, 2003
Accepted: August 25, 2003
Published: September 18, 2003

References

Asao, H., Sasaki, Y., Arita, T., Tanaka, N., Endo, K., Kasai, H., Takeshita, T., Endo, Y., Fujita, T., and Sugamura, K. (1997). Hrs is associated with STAM, a signal-transducing adaptor molecule. Its suppressive effect on cytokine-induced cell growth. J. Biol. Chem. *272*, 32785–32791.

Babst, M., Odorizzi, G., Estepa, E.J., and Emr, S.D. (2000). Mammalian tumor susceptibility gene 101 (TSG101) and the yeast homologue, Vps23p, both function in late endosomal trafficking. Traffic *1*, 248–258.

Babst, M., Katzmann, D., Estepa-Sabal, E., Meerloo, T., and Emr, S. (2002a). Escrt-III: an endosome-associated heterooligomeric protein complex required for mvb sorting. Dev. Cell *3*, 271–282.

Babst, M., Katzmann, D., Snyder, W., Wendland, B., and Emr, S. (2002b). Endosome-associated complex, ESCRT-II, recruits trans-

port machinery for protein sorting at the multivesicular body. Dev. Cell *3*, 283–289.

Bache, K.G., Brech, A., Mehlum, A., and Stenmark, H. (2003a). Hrs regulates multivesicular body formation via ESCRT recruitment to endosomes. J. Cell Biol. *162*, 435–442.

Bache, K.G., Raiborg, C., Mehlum, A., and Stenmark, H. (2003b). STAM and Hrs are subunits of a multivalent ubiquitin-binding complex on early endosomes. J. Biol. Chem. *278*, 12513–12521.

Basyuk, E., Galli, T., Mougel, M., Blanchard, J.M., Sitbon, M., and Bertrand, E. (2003). Retroviral genomic RNAs are transported to the plasma membrane by endosomal vesicles. Dev. Cell *5*, 161–174.

Biscone, M.J., Pierson, T.C., and Doms, R.W. (2002). Opportunities and challenges in targeting HIV entry. Curr. Opin. Pharmacol. *2*, 529–533.

Bishop, N., and Woodman, P. (2001). TSG101/mammalian VPS23 and mammalian VPS28 interact directly and are recruited to VPS4-induced endosomes. J. Biol. Chem. *276*, 11735–11742.

Bishop, N., Horman, A., and Woodman, P. (2002). Mammalian class E vps proteins recognize ubiquitin and act in the removal of endosomal protein-ubiquitin conjugates. J. Cell Biol. *157*, 91–101.

Chatellard-Causse, C., Blot, B., Cristina, N., Torch, S., Missotten, M., and Sadoul, R. (2002). Alix (ALG-2-interacting protein X), a protein involved in apoptosis, binds to endophilins and induces cytoplasmic vacuolization. J. Biol. Chem. *277*, 29108–29115.

Cook, R.F., Leroux, C., Cook, S.J., Berger, S.L., Lichtenstein, D.L., Ghabrial, N.N., Montelaro, R.C., and Issel, C.J. (1998). Development and characterization of an in vivo pathogenic molecular clone of equine infectious anemia virus. J. Virol. *72*, 1383–1393.

Demirov, D.G., Ono, A., Orenstein, J.M., and Freed, E.O. (2002a). Overexpression of the N-terminal domain of TSG101 inhibits HIV-1 budding by blocking late domain function. Proc. Natl. Acad. Sci. USA *99*, 955–960.

Demirov, D.G., Orenstein, J.M., and Freed, E.O. (2002b). The late domain of human immunodeficiency virus type 1 p6 promotes virus release in a cell type-dependent manner. J. Virol. *76*, 105–117.

Denzer, K., Kleijmeer, M.J., Heijnen, H.F., Stoorvogel, W., and Geuze, H.J. (2000). Exosome: from internal vesicle of the multivesicular body to intercellular signaling device. J. Cell Sci. *113*, 3365–3374.

Dettenhofer, M., and Yu, X.F. (1999). Highly purified human immunodeficiency virus type 1 reveals a virtual absence of Vif in virions. J. Virol. *73*, 1460–1467.

Freed, E.O. (2002). Viral late domains. J. Virol. *76*, 4679–4687.

Fujita, H., Yamanaka, M., Imamura, K., Tanaka, Y., Nara, A., Yoshimori, T., Yokota, S., and Himeno, M. (2003). A dominant negative form of the AAA ATPase SKD1/VPS4 impairs membrane trafficking out of endosomal/lysosomal compartments: class E vps phenotype in mammalian cells. J. Cell Sci. *116*, 401–414.

Garrus, J.E., von Schwedler, U.K., Pornillos, O.W., Morham, S.G., Zavitz, K.H., Wang, H.E., Wettstein, D.A., Stray, K.M., Cote, M., Rich, R.L., et al. (2001). Tsg101 and the vacuolar protein sorting pathway are essential for HIV-1 budding. Cell *107*, 55–65.

Göttlinger, H.G., Dorfman, T., Sodroski, J.G., and Haseltine, W.A. (1991). Effect of mutations affecting the p6 gag protein on human immunodeficiency virus particle release. Proc. Natl. Acad. Sci. USA *88*, 3195–3199.

Gould, S.J., Booth, A.M., and Hildreth, J.E.K. (2003). The Trojan exosome hypothesis. Proc. Natl. Acad. Sci. USA *100*, 10592–10597.

Gross, I., Hohenberg, H., and Krausslich, H.G. (1997). In vitro assembly properties of purified bacterially expressed capsid proteins of human immunodeficiency virus. Eur. J. Biochem. *249*, 592–600.

Hermida-Matsumoto, L., and Resh, M.D. (2000). Localization of human immunodeficiency virus type 1 Gag and Env at the plasma membrane by confocal imaging. J. Virol. *74*, 8670–8679.

Howard, T.L., Stauffer, D.R., Degnin, C.R., and Hollenberg, S.M. (2001). CHMP1 functions as a member of a newly defined family of vesicle trafficking proteins. J. Cell Sci. *114*, 2395–2404.

Igakura, T., Stinchcombe, J.C., Goon, P.K., Taylor, G.P., Weber, J.N., Griffiths, G.M., Tanaka, Y., Osame, M., and Bangham, C.R. (2003). Spread of HTLV-I between lymphocytes by virus-induced polarization of the cytoskeleton. Science *299*, 1713–1716.

Kamura, T., Burian, D., Khalili, H., Schmidt, S.L., Sato, S., Liu, W.J., Conrad, M.N., Conaway, R.C., Conaway, J.W., and Shilatifard, A. (2001). Cloning and characterization of ELL-associated proteins EAP45 and EAP20. A role for yeast EAP-like proteins in regulation of gene expression by glucose. J. Biol. Chem. *276*, 16528–16533.

Katzmann, D.J., Odorizzi, G., and Emr, S.D. (2002). Receptor down-regulation and multivesicular-body sorting. Nat. Rev. Mol. Cell Biol. *3*, 893–905.

Katzmann, D.J., Stefan, C.J., Babst, M., and Emr, S.D. (2003). Vps27 recruits ESCRT machinery to endosomes during MVB sorting. J. Cell Biol. *162*, 413–423.

Licata, J.M., Simpson-Holley, M., Wright, N.T., Han, Z., Paragas, J., and Harty, R.N. (2003). Overlapping motifs (PTAP and PPEY) within the Ebola virus VP40 protein function independently as late budding domains: involvement of host proteins TSG101 and VPS-4. J. Virol. *77*, 1812–1819.

Lu, Q., Hope, L.W., Brasch, M., Reinhard, C., and Cohen, S.N. (2003). TSG101 interaction with HRS mediates endosomal trafficking and receptor down-regulation. Proc. Natl. Acad. Sci. USA *100*, 7626–7631.

Martin-Serrano, J., Zang, T., and Bieniasz, P.D. (2001). HIV-1 and Ebola virus encode small peptide motifs that recruit Tsg101 to sites of particle assembly to facilitate egress. Nat. Med. *7*, 1313–1319.

Martin-Serrano, J., Zang, T., and Bieniasz, P.D. (2003). Role of ESCRT-I in retroviral budding. J. Virol. *77*, 4794–4804.

McDonald, D., Wu, L., Bohks, S.M., KewalRamani, V.N., Unutmaz, D., and Hope, T.J. (2003). Recruitment of HIV and its receptors to dendritic cell-T cell junctions. Science *300*, 1295–1297.

Muller, B., Patschinsky, T., and Krausslich, H.G. (2002). The late-domain-containing protein p6 is the predominant phosphoprotein of human immunodeficiency virus type 1 particles. J. Virol. *76*, 1015–1024.

Odorizzi, G., Katzmann, D.J., Babst, M., Audhya, A., and Emr, S.D. (2003). Bro1 is an endosome-associated protein that functions in the MVB pathway in Saccharomyces cerevisiae. J. Cell Sci. *116*, 1893–1903.

Ott, D.E., Coren, L.V., Johnson, D.G., Kane, B.P., Sowder, R.C., 2nd, Kim, Y.D., Fisher, R.J., Zhou, X.Z., Lu, K.P., and Henderson, L.E. (2000). Actin-binding cellular proteins inside human immunodeficiency virus type 1. Virology *266*, 42–51.

Pelchen-Matthews, A., Kramer, B., and Marsh, M. (2003). Infectious HIV-1 assembles in late endosomes in primary macrophages. J. Cell Biol. *162*, 443–455.

Pornillos, O., Alam, S., Rich, R.L., Myszka, D.G., Davis, D.R., and Sundquist, W.I. (2002a). Structure and functional interactions of the Tsg101 UEV domain. EMBO J. *21*, 2397–2406.

Pornillos, O., Alam, S.L., Davis, D.R., and Sundquist, W.I. (2002b). Structure of the Tsg101 UEV domain in complex with the PTAP motif of the HIV-1 p6 protein. Nat. Struct. Biol. *9*, 812–817.

Pornillos, O.P., Garrus, J.E., and Sundquist, W.I. (2002c). Mechanisms of enveloped RNA virus budding. Trends Cell Biol. *12*, 569–579.

Pornillos, O., Higginson, D.S., Stray, K.M., Fisher, R.D., Garrus, J.E., Payne, M., He, G.P., Wang, H.E., Morham, S.G., and Sundquist, W.I. (2003). HIV Gag mimics the Tsg101-recruiting activity of the human Hrs protein. J. Cell Biol. *162*, 425–434.

Puffer, B.A., Parent, L.J., Wills, J.W., and Montelaro, R.C. (1997). Equine infectious anemia virus utilizes a YXXL motif within the late assembly domain of the Gag p9 protein. J. Virol. *71*, 6541–6546.

Puffer, B.A., Watkins, S.C., and Montelaro, R.C. (1998). Equine infectious anemia virus Gag polyprotein late domain specifically recruits cellular AP-2 adapter protein complexes during virion assembly. J. Virol. *72*, 10218–10221.

Raposo, G., Moore, M., Innes, D., Leijendekker, R., Leigh-Brown, A., Benaroch, P., and Geuze, H. (2002). Human macrophages accumulate HIV-1 particles in MHC II compartments. Traffic *3*, 718–729.

Scheuring, S., Rohricht, R.A., Schoning-Burkhardt, B., Beyer, A.,

Muller, S., Abts, H.F., and Kohrer, K. (2001). Mammalian cells express two VPS4 proteins both of which are involved in intracellular protein trafficking. J. Mol. Biol. *312*, 469–480.

Sherer, N.M., Lehmann, M.J., Jimenez-Soto, L.F., Ingmundson, A., Haner, S.M., Cicchetti, G., Allen, P.G., Pypaert, M., Cunningham, J.A., and Mothes, W. (2003). Visualization of retroviral replication in living cells reveals budding into multivascular bodies. Traffic, in press.

Strack, B., Calistri, A., Craig, S., Popova, E., and Göttlinger, H.G. (2003). AIP1/ALIX is a binding partner for HIV-1 p6 and EIAV p9 functioning in virus budding. Cell, *114*, 689–699.

Thery, C., Boussac, M., Veron, P., Ricciardi-Castagnoli, P., Raposo, G., Garin, J., and Amigorena, S. (2001). Proteomic analysis of dendritic cell-derived exosomes: a secreted subcellular compartment distinct from apoptotic vesicles. J. Immunol. *166*, 7309–7318.

VerPlank, L., Bouamr, F., LaGrassa, T.J., Agresta, B., Kikonyogo, A., Leis, J., and Carter, C.A. (2001). Tsg101, a homologue of ubiquitin-conjugating (E2) enzymes, binds the L domain in HIV type 1 Pr55Gag. Proc. Natl. Acad. Sci. USA *98*, 7724–7729.

Vincent, O., Rainbow, L., Tilburn, J., Arst Jr, H.N., Jr., and Penalva, M.A. (2003). YPXL/I Is a protein interaction motif recognized by aspergillus PalA and its human homologue, AIP1/Alix. Mol. Cell. Biol. *23*, 1647–1655.

von Schwedler, U.K., Stemmler, T.L., Klishko, V.Y., Li, S., Albertine, K.H., Davis, D.R., and Sundquist, W.I. (1998). Proteolytic refolding of the HIV-1 capsid protein amino-terminus facilitates viral core assembly. EMBO J. *17*, 1555–1568.

Welker, R., Hohenberg, H., Tessmer, U., Huckhagel, C., and Krausslich, H.G. (2000). Biochemical and structural analysis of isolated mature cores of human immunodeficiency virus type 1. J. Virol. *74*, 1168–1177.